Article

Thermodynamics of DNA Hybridization on Gold Nanoparticles

Jun Xu, and Stephen L. Craig

J. Am. Chem. Soc., **2005**, 127 (38), 13227-13231• DOI: 10.1021/ja052352h • Publication Date (Web): 01 September 2005

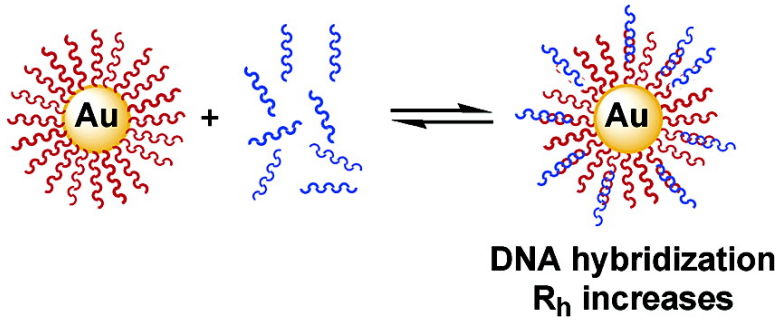

More About This Article

Additional resources and features associated with this article are available within the HTML version:

- Supporting Information
- Links to the 7 articles that cite this article, as of the time of this article download
- Access to high resolution figures
- Links to articles and content related to this article
- Copyright permission to reproduce figures and/or text from this article

View the Full Text HTML

J|A|C|S
ARTICLES
Published on Web 09/01/2005

Thermodynamics of DNA Hybridization on Gold Nanoparticles

Jun Xu and Stephen L. Craig*

Contribution from the Department of Chemistry and Center for Biologically Inspired Materials and Material Systems, Duke University, Durham, North Carolina 27708-0346

Received April 11, 2005; E-mail: stephen.craig@duke.edu

Abstract: Dynamic light scattering is used as a sensitive probe of hybridization on DNA-functionalized colloidal gold nanoparticles. When a target DNA strand possesses an 8 base "dangling end", duplex formation on the surface of the nanoparticles leads to an increase in hydrodynamic radius. Duplex melting is manifested in a drop in hydrodynamic radius with increasing temperature, and the concentration dependence of the melting temperature provides a measure of the thermodynamics of binding. The hybridization thermodynamics are found to be significantly lower at higher hybridization densities than those previously reported for initial hybridization events. The pronounced deviation from Langmuir adsorption behavior is greater for longer duplexes, and it is, therefore, consistent with electrostatic repulsion between densely packed oligonucleotides. The results have implications for sensing and DNA-directed nanoparticle assembly.

Introduction

DNA-functionalized colloidal gold nanoparticles (DNA−Au) hold promise for applications in nanotechnology and biotechnology.[1] Following the pioneering work of Mirkin and co-workers, these modified nanoparticles can act as useful building blocks to form spatially well-defined superstructures, including nanocrystals,[2] binary[3] and multilayered[4] nanoparticle assemblies, and well-ordered three-dimensional nanoclusters.[5] More importantly, DNA-functionalized gold colloids have been widely used to develop highly sensitive biosensors. Mirkin and co-workers have reported selective colorimetric detection of DNA up to one single mismatch[6] and an ultrasensitive scanometric DNA array detection.[7] Maeda reported later that aggregation can be triggered by non-crosslinking DNA hybridization, and that the technique is also capable of single mismatch discrimination.[8] Increasing research efforts in DNA−Au-based biosensors have expanded the application of DNA−Au to other DNA detection techniques, such as the quartz crystal microbalance[4b,9] and surface plasmon resonance,[10] as well as to the detection of other biomolecules, such as proteins.[11]

The thermodynamics of individual DNA hybridization events on DNA−Au are central to these applications, but surprisingly, little information about those thermodynamics is available. Mirkin and Schatz[12] have shown that DNA−Au aggregates are more stable than the isolated duplexes, and a detailed study has revealed the importance of cooperativity, probe density on the nanoparticle surface, gold nanoparticle size, salt concentration, and interparticle distance. In that work, the effect of multiple hybridization events on DNA−Au is shown to increase the thermodynamic stability of the aggregates through cooperative binding, although delineating the contributions of cooperativity from the strength of the individual hybridization events, considered in the absence of cooperative aggregation, is challenging.

The hybridization thermodynamics of immobilized dsDNA have been investigated recently in the context of functionalized planar silicon[13] and gold[10c,14] surfaces—an area of current interest because of its importance to microarray technology. The hybridization behavior on such surfaces often differs from that in bulk solution, although the details of that behavior are often

(1) For related reviews, see: (a) Niemeyer, C. M. *Angew. Chem., Int. Ed.* **2001**, *40*, 4128−4158. (b) Storhoff, J. J.; Mirkin, C. A. *Chem. Rev.* **1999**, *99*, 1849−1862. (c) Shipway, A. N.; Willner, I. *Chem. Commun.* **2001**, 2035−2045.
(2) (a) Alivisatos, A. P.; Johnsson, K. P.; Peng, X.; Wilson, T. E.; Loweth, C. J.; Bruchez, M. P., Jr.; Schultz, P. G. *Nature* **1996**, *382*, 609−611. (b) Deng, Z.; Tian, Y.; Lee, S. H.; Ribbe, A.; Mao, C. *Angew. Chem., Int. Ed.* **2005**, *44*, 3582−3585.
(3) (a) Mucic, R. C.; Storhoff, J. J.; Mirkin, C. A.; Letsinger, R. L. *J. Am. Chem. Soc.* **1998**, *120*, 12674−12675. (b) Zou, B.; Ceyhan, B.; Simon, U.; Niemeyer, C. M. *Angew. Chem., Int. Ed.* **2005**, *17*, 1643−1647.
(4) (a) Taton, T. A.; Mucic, R. C.; Mirkin, C. A.; Letsinger, R. L. *J. Am. Chem. Soc.* **2000**, *122*, 6305−6306. (b) Patolsky, F.; Ranjit, K. T.; Lichtenstein, A.; Willner, I. *Chem. Commun.* **2000**, 1025−1026.
(5) Mirkin, C. A.; Letsinger, R. L.; Mucic, R. C.; Storhoff, J. J. *Nature* **1996**, *382*, 607−609.
(6) Elghanian, R.; Storhoff, J. J.; Mucic, R. C.; Letsinger, R. L.; Mirkin, C. A. *Science* **1997**, *277*, 1078−1081.
(7) Taton, T. A.; Mirkin, C. A.; Letsinger, R. L. *Science* **2000**, *289*, 1757−1760.
(8) Sato, K.; Hosokawa, K.; Maeda, M. *J. Am. Chem. Soc.* **2003**, *125*, 8102−8103.
(9) (a) Han, S.; Lin, J.; Satjapipat, M.; Baca, A. J.; Zhou, F. *Chem. Commun.* **2001**, 609−610. (b) Su, X.; Li, S. F. Y.; O'shea, S. J. *Chem. Commun.* **2001**, 755−756. (c) Lin, L.; Zhao, H.-Q.; Li, J.-R.; Tang, J.-A.; Duan, M.-X.; Jiang, L. *Biochem. Biophys. Res. Commun.* **2000**, *274*, 817−820.
(10) (a) Goodrich, T. T.; Lee, H. J.; Corn, R. M. *J. Am. Chem. Soc.* **2004**, *126*, 4086−4087. (b) He, L.; Musick, M. D.; Nicewarner, S. R.; Salinas, F. G.; Benkovic, S. J.; Natan, M. J.; Keating, C. D. *J. Am. Chem. Soc.* **2000**, *122*, 9071−9077. (c) Peterlinz, K. A.; Georgiadis, R. M. *J. Am. Chem. Soc.* **1997**, *119*, 3401−3402.
(11) Nam, J.-M.; Thaxton, C. S.; Mirkin, C. A. *Science* **2003**, *301*, 1884−1886.
(12) Jin, R.; Wu, G.; Li, Z.; Mirkin, C. A.; Schatz, G. C. *J. Am. Chem. Soc.* **2003**, *125*, 1643−1654.
(13) (a) Piunno, P. A. E.; Watterson, J.; Wust, C. C.; Krull, U. J. *Anal. Chim. Acta* **1999**, *400*, 73−89. (b) Marquette, C. A.; Lawrence, I.; Polychronakos, C.; Lawrence, M. F. *Talanta* **2002**, *56*, 763−768.
(14) Meunier-Prest, R.; Raveau, S.; Finot, E.; Legay, G.; Cherkaoui-Malki, M.; Latruffe, N. *Nucleic Acids Res.* **2003**, *31*, e150.

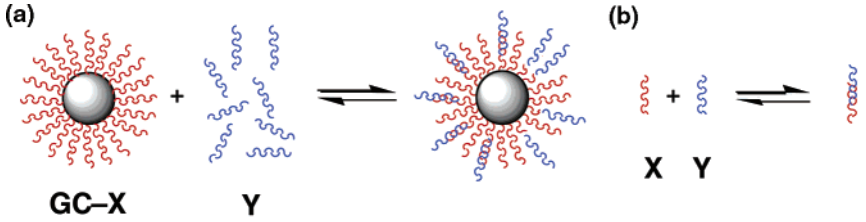

Figure 1. Pictorial representation of hybridization (a) on a DNA-modified gold nanoparticle and (b) in solution. Hybridization of a complement bearing a dangling end increases the hydrodynamic radius of the nanoparticle and can be followed by dynamic light scattering. X represents oligonucleotides **1**−**3**, and Y represents oligonucleotides **4**−**7** in Table 1.

Table 1. Oligonucleotide Samples and Their Nucleobase Sequences

oligo	base sequence (5′ to 3′)
1	HS−$(CH_2)_6$−TCTACCAC
2	HS−$(CH_2)_6$−TAATTCTACCAC
3	HS−A_{10}−ATCCTTTACAATATT
4	AGAGAGCCGTGGTAGA
5	AGAGAGCCGTGGTAGAATTA
6	AGAGAGCCGTGGTAGAAGTA
7	AGAGAGCCAATATTGTAAAGGAT

case-specific; duplex stability may be greater than or weaker than that in solution. Extrapolating the findings on planar surfaces to small particles is complicated by the relatively high curvature of the DNA−Au surface, which relaxes the steric and electrostatic interactions between neighboring DNA and may also perturb long-range interactions. We report here that dynamic light scattering (DLS) provides a surprisingly sensitive probe of DNA hybridization on nanoparticle surfaces. The enthalpy and entropy of duplex formation on partially hybridized DNA−Au are found to be muted significantly relative to their values in solution.

Experimental Section

Materials: Oligonucleotides (Table 1) were purchased from Operon Biotechnologies and Integrated DNA Technologies Inc., except **3** (**GC-3** was generously provided by A. Lytton-Jean and C. Mirkin). Oligonucleotides **1**−**2** were received as disulfides and were reduced by solid-phase DTT (Calbiochem Inc.), followed by desalting through Poly-Pack cartridges (Glen Research Corp.) prior to gold surface modification. Oligonucleotides **4**−**7** were used as received. Gold colloids (10 nm in diameter) were purchased from Ted Pella Inc. and used as received.

DNA−Au Preparation. Solutions of DNA−Au were prepared according to previously reported procedures[7,8] with minor modifications. Briefly, 5 nmol oligonucleotide **1** or **2** was mixed with 1 mL of gold colloids (10 nM) and incubated at 50 °C for 1 day. The solution was then changed to 0.1 M NaCl, 10 mM phosphate buffer, pH 7, and was kept at 50 °C for another 2 days. Excess **1** or **2** was removed from modified gold colloids as follows: the mixture was centrifuged at 20 000 rpm for 40 min; the supernatant was decanted, and the residue was redispersed in 0.1 M NaCl, 10 mM phosphate buffer, pH 7. This procedure was repeated again, but the final reddish residue was dispersed in 0.3 M PBS buffer (0.3 M NaCl, 10 mM phosphate buffer, pH 7) and filtered through 100 nm pore size membrane. The concentration of modified gold colloids was determined by UV absorbance at 530 nm using a molar extinction coefficient of 1.056×10^8 M^{-1} cm^{-1} (Ted Pella Inc.).

Dynamic Light Scattering. DNA thermodynamics on the gold nanoparticle surfaces were determined by dynamic light scattering. Gold colloids modified by **1** or **2** (termed **GC-1** and **GC-2**, 4 nM) were mixed with **4** or **5** at different concentrations (0.01, 0.03, 0.10, 0.20 mM). Sample solutions were annealed at 80 °C for 10 min and then filtered through a 100 nm nanofilter (Protein-Solutions) into a microcuvette. Dynamic light scattering measurements were conducted using a DAWN EOS MALS (Wyatt Technology) with a quasi-elastic detector positioned at 108° with respect to the direction of the laser beam. The solution was heated or cooled at 1 °C/min and equilibrated for 30 min at each temperature of interest. Light scattering correlation functions were collected using ASTRA software (Wyatt Technology) and processed with QELSBatch software (Wyatt Technology) to obtain the hydrodynamic radii. The measurement was repeated multiple times, and at least 30 values were obtained to give an average hydrodynamic radius.

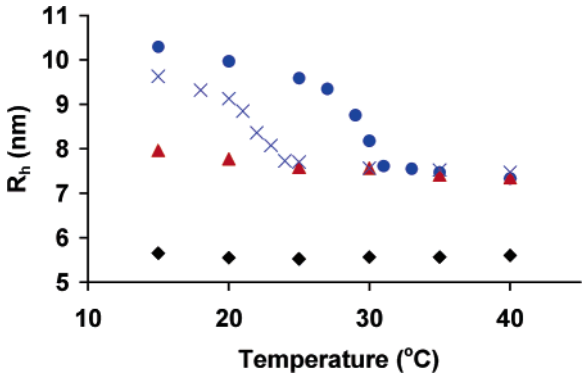

Figure 2. Hydrodynamic radius (R_h) versus temperature for bare gold colloids (◆), **GC-1** (▲), 4 nM **GC-1** + 0.01 mM **4** (×), 4 nM **GC-1** + 0.10 mM **4** (●).

UV−Vis Spectrophotometry. DNA thermodynamics in solution were determined using a Hewlett-Packard 845x UV−visible spectrophotometer according to literature procedures.[15] DNA thermal melting curves were measured at 260 nm from 20 to 70 °C with 0.5 °C/min ramping rate, and five different concentrations were used, typically from 1 to 17 μM in 0.3 M PBS buffer. Thermodynamic parameters were extrapolated from the plot of $1/T_m$ versus $\ln(C)$, where C is the total concentration of oligonucleotides (Supporting Information).

Results and Discussion

Dynamic light scattering (DLS) was used to observe DNA hybridization on the gold nanoparticle surfaces, as described schematically in Figure 1. Initial measurements in the absence of the hybridizing target strand (blue, Figure 1) were used to characterize the DNA−Au and set a baseline for the hybridization experiments. The hydrodynamic radius, R_h, of the unfunctionalized bare gold colloids was measured by DLS to be 5.5 nm, in good agreement with the supplier's provided mean diameter of 9.9 nm (Figure 2). After treatment with oligonucleotide thiol **1**, the R_h of the modified nanoparticle **GC-1** increases to 7.6 nm due to the added oligonucleotide (Figure 2). A 3.2 nm increase was observed in **GC-2** (data not shown), functionalized with the longer thiol **2**, indicating that the oligos extend away from the particle surface.

(15) Plum, G. E.; Breslauer, K. J.; Roberts, R. W. *Comp. Nat. Prod. Chem.* **1999**, *7*, 15−53.

Duplex formation was monitored through further changes in R_h. Nanoparticle **GC-1** was mixed with an excess (0.01−0.20 mM) of complementary oligonucleotide **4**. Upon hybridization, the dangling, unpaired 8 bases of **4** lead to an increase of ∼2 nm in R_h that can be monitored by DLS. The hydrodynamic radius decreased with increasing temperature, as reported in Figure 2. The reversible transition was reproduced three times for a single sample, and it was not observed with either the bare gold or DNA−Au alone, suggesting that the change in R_h is due to duplex melting. The melting temperature (T_m, defined by the midpoint[16] of the change in R_h) depends on the concentration of complementary DNA in solution, providing additional evidence that hybridization and not conformational change within the DNA−Au is responsible.[15]

The concentration dependence of the melting temperature reflects the thermodynamics of hybridization. At T_m, some fraction ϕ of the available binding sites on the DNA−Au surface are occupied, and the equilibrium constant for hybridization, K_{hyb}, is given by eq 1:

$$K_{hyb} = [ds]_{Au}/([ss]_{Au}[ss]_{sol}) = \phi/((1 - \phi)[ss]_{sol}) \quad (1)$$

where $[ds]_{Au}$ and $[ss]_{Au}$ are the concentration of double-stranded and single-stranded DNA on the DNA−Au surface, respectively, and $[ss]_{sol}$ is the concentration of single-stranded target DNA in solution. At T_m, $\phi = 0.5$ is an upper bound for the fraction of bound sites, complementary fluorescence measurements provide a lower bound of $\phi = 0.1$,[17] and so the DLS melting curves can be treated similarly to typical UV melting curves, and a plot of $1/T_m$ versus $[ss]_{sol}$ gives both the enthalpy and entropy of hybridization (examples in Figure 3). The uncertainty of a factor of ∼10 in K_{hyb}, a result of the uncertainty in ϕ, is likely to be systematic, however, because of the similarity in the structures of the DNA−Au and consistent use of an 8 base dangling end. As a result, the relative uncertainties between measurements are significantly less than the uncertainties in the individual measurements reported throughout this paper.

For **GC-1** + **4**, the apparent free energy of hybridization at 298 K is −5.4 kcal mol^{-1}. By comparison, standard UV melting studies reveal that the free energy of the same DNA hybridization in solution (**1** + **4**) is −8.9 kcal mol^{-1}; the 3.5 kcal mol^{-1} difference in free energy of hybridization for the same duplex on the nanoparticle surface versus that in solution is denoted ΔG_{diff}. As we discuss below, ΔG_{diff} is specific for the measurement at hand because hybridization thermodynamics depend on surface coverage. Nonetheless, ΔG_{diff} provides a measure of the destabilization that can be compared from one experiment to the next and facilitates a discussion of observed trends. The apparently lower T_m values could be the result of heating from the laser light irradiation, which could cause the DNA−Au sample to experience a higher temperature than is regulated by the temperature controller. To determine whether heating from the laser affects the measurement, the laser was turned off during the temperature equilibration and then turned on immediately (<10 s) before commencing data collection. We find no significant difference between either the appearance of the correlation function or the measured values of R_h at the beginning of data collection and those at the end (30 min), indicating that laser irradiation at the wavelength and powers used here does not make a significant contribution to the observed differences in thermodynamics (Supporting Information). Additionally, the shape of the correlation functions, as well as the good agreement between the observed and expected values of R_h, suggests that thermal lensing[18] does not significantly contribute to the measurements.

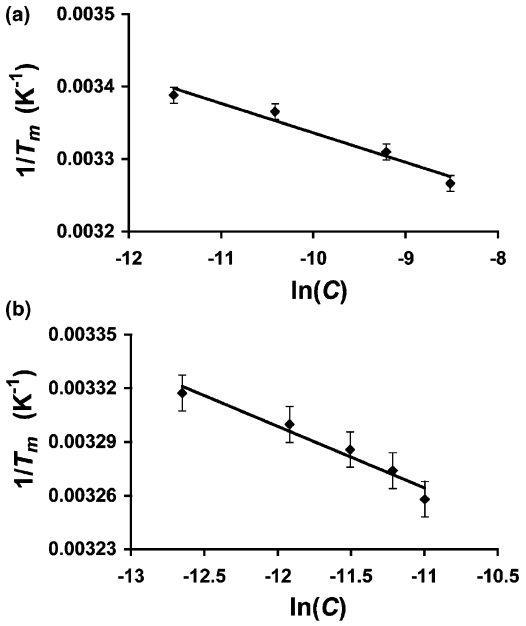

Figure 3. Representative plots for the determination of DNA thermodynamics (a) on gold nanoparticle surface, where T_m values are taken from dynamic light scattering (**GC-1** + **4**) and C is the concentration in mol L^{-1} of target DNA in solution, and (b) in 0.3 M PBS buffer solution, where T_m is taken from UV spectroscopy (**1** + **4**) and C is the total concentration of oligonucleotide in mol L^{-1}. Error bars reflect an uncertainty of ±1 °C in the individual melting temperatures.

At the molecular level, the physical basis for the observed destabilization is likely to comprise contributions from two primary effects: the electrostatic repulsion between neighboring hybridized DNA target strands (Y and Y, Figure 1a), and the electrostatic repulsion between the hybridized DNA target strands and the negatively charged gold surface (Y and X, Figure 1b). To address these contributions, the hybridization thermodynamics were determined for **GC-2** + **4**, where four additional unpaired bases increase the charge density of **GC-2** versus **GC-1**. The value of ΔG_{diff} = 3.6 kcal mol^{-1} in **GC-2** + **4** is experimentally indistinguishable from that of **GC-1** + **4**, implying that electrostatic repulsion between the target and the negatively charged DNA−Au is not the primary determinant of the destabilization. The electrostatic repulsion between target strands might thus dominate the destabilization. Further support of this conclusion is found in recent work by Mirkin,[19] who has shown by fluorescence quenching that, on a statistical basis, early hybridization events are not significantly perturbed from those in solution. We note that the destabilization observed in

(16) The melting curves from light scattering cannot be treated identically to those from a traditional UV−vis experiment because of the uncertainty in ϕ. If T_m as defined occurs at $\phi = 0.5$, the treatments become identical. If, however, the midpoint of the transition occurs at a lower value (we are unaware of any explanation that would permit a higher value of ϕ at T_m), the resulting error is systematic and small—if the midpoint reflects only 9% hybridization, the effective thermodynamics are systematically *overestimated* by 1.4 kcal mol^{-1}, and the destabilization is *underestimated* by a comparable amount. These factors are taken into account in the values and uncertainties reported in the main text.

(17) Xu, J.; Craig, S. L. Unpublished results.

(18) (a) Navas, M. J.; Jimenez, A. M. *Crit. Rev. Anal. Chem.* **2003**, *33*, 77−88. (b) Rashidi-Huyeh, M.; Palpant, B. *J. Appl. Phys.* **2004**, *96*, 4475−4482.

(19) Lytton-Jean, A. K. R.; Mirkin, C. A. *J. Am. Chem. Soc.* **2005**, in press.

Table 2. DNA Hybridization Thermodynamics on Gold Colloids (GC) and in Solution. Thermodynamics of Hybridization on the Gold Colloids Are Apparent Values Based on Melting Temperatures Defined by a 50% Decrease in Hydrodynamic Radius

	ΔH (kcal mol^{-1})[a]	ΔS (cal mol^{-1}K^{-1})[a]	ΔG_{298} (kcal mol^{-1})[a]	ΔG_{diff} (kcal mol^{-1})
GC-1 + 4	−48.8 ± 7.8	−145 ± 28	−5.4 ± 0.8	3.5 ± 1.2
1 + 4	−57.9 ± 19.6	−167 ± 65	−8.9 ± 0.4	
GC-2 + 4	−49.2 ± 7.9	−146 ± 28	−5.7 ± 0.8	3.6 ± 1.1
2 + 4	−62.5 ± 15.6	−181 ± 51	−9.3 ± 0.3	
GC-2 + 5	−50.7 ± 6.4	−149 ± 23	−6.2 ± 0.8	5.5 ± 1.5
2 + 5	−60.4 ± 14.3	−166 ± 45	−11.7 ± 0.8	
GC-2 + 6	−44.5 ± 6.6	−132 ± 25	−5.2 ± 0.8	4.8 ± 1.3
2 + 6	−58.1 ± 12.9	−164 ± 42	−10.0 ± 0.5	
GC-3 + 7	−66.2 ± 20.1	−194 ± 68	−8.3 ± 1.3	8.4 ± 3.3
3 + 7			−16.7 ± 2.0[b]	

[a] Uncertainties reflect an uncertainty of ±1 °C in the individual T_m measurements; these uncertainties lead to compensating changes in ΔH and ΔS, and as a result, uncertainties in ΔG are quite small. Deviation in the linear least-squares fits is considerably smaller. The uncertainties in the relative values of ΔG_{298} and ΔG_{diff} are 0.7 kcal mol^{-1} smaller than those of the absolute values. [b] Value taken from ref 19 with kind permission. This free energy value is reported for oligonucleotides with a fluorophore at the 5′ end of **3** and a quencher at the 3′ end of **7**, and there is no 8 base dangling end on **7**.

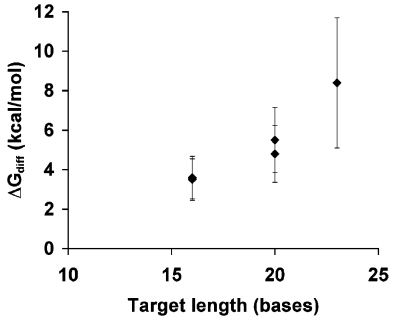

Figure 4. The dependence of ΔG_{diff} on the length of hybridized oligonucleotide target strand (represented by the number of bases). Error bars reflect uncertainties in the absolute values of ΔG_{diff}, relative uncertainties are ∼0.7 kcal mol^{-1} smaller.

our experiments is characterized by roughly similar decreases in the magnitude of both the enthalpy and entropy of hybridization (Table 2).

It is further found that ΔG_{diff} increases with hybridized duplex length. For example, **GC-2 + 5** possesses a complementary 12 base overlap while maintaining the same dangling end found in **GC-2 + 4**. Hybridization thermodynamics on the surface and in solution increase relative to those in **GC-2 + 4**, but ΔG_{diff} increases to 5.5 kcal mol^{-1} versus 3.5 kcal mol^{-1} for the 8 base overlaps (Table 2). When a single mismatch is introduced within the 12 base overlap (**GC-2 + 6**), the thermodynamics of hybridization are lower than those observed in **GC-2 + 5**, but a similar ΔG_{diff} of 4.8 kcal mol^{-1} is observed (Table 2).

To test the importance of particle preparation, we repeated our measurements on **GC-3**, a 13 nm gold particle with an A_{10} spacer that is known to increase the stability of hybridization-induced aggregates. The 15 base overlap with **7** is destabilized from −16.7 kcal mol^{-1} (measured with attached fluorophore and quencher)[19] to −9.7 kcal mol^{-1}. Although the fluorophore and quencher may increase the hybridization thermodynamics in solution, it is clear that ΔG_{diff} is greater for the longer duplex than for the 8-mer or 12-mer overlaps. Figure 4 summarizes the relationship between the ΔG_{diff} and target strand length. If the energy destabilization is caused primarily by electrostatic repulsion between hybridized target strands, ΔG_{diff} would be expected to increase as the square of the target oligonucleotide length, and for the data obtained $\Delta G_{diff} \sim$ (number of bases)$^{2.1}$. The good agreement in the scaling belies what is, in fact, an oversimplification of a far more complex picture. Vainrub and Pettitt[20] have pointed out the complexities of the electrostatics in planar DNA surface arrays, and the data obtained are simply not capable of delineating more subtle contributions, such as those from the curvature of the gold nanoparticle surface, which should alleviate electrostatic repulsion in longer duplexes, and those from electrostatic interactions between the target strands and the DNA−Au probe strands.

Lytton-Jean and Mirkin have used fluorescence-based studies of **GC-3** and related systems to demonstrate that an entire DNA−Au particle is collectively a stronger binder of target DNA than is an isolated, complementary sequence in solution.[19] Normalizing for the statistics of the DNA−Au multivalency (∼100/particle), their results show that hybridization thermodynamics at low levels of surface hybridization are comparable in stability to those in solution on a strand-per-strand basis. The thermodynamics observed here are far weaker; the melting observed by DLS is complete at temperatures for which the hybridization efficiency would be >99% in solution. A likely explanation is that, in the present work, the measured T_m occurs at a significant degree (10−50%) of surface hybridization. Duplexes on the DNA−Au surface may destabilize nearby duplexes through Coulomb blockage, leading to non-Langmuir isotherms,[20] and the observed melting curves are consistent with that behavior. For **GC-2 + 5**, the magnitude of the destabilization is within a factor of roughly 2 of that computed using isotherms developed by Vainrub for probes immobilized on planar surfaces.[20,23] Fluorescence quenching experiments, similar to those carried out by Lytton-Jean and Mirkin, as a function of target:DNA−Au ratio confirm that destabilization increases significantly with surface coverage; the T_m drops 4 °C with only 4−5 strands bound per DNA−Au.[17] Even on very small nanoparticles with high curvature or relatively long spacers between the gold surface and binding sequence, therefore, hybridization cannot be regarded as a series of independent events. The thermodynamics reported in Table 2 are, therefore,

(20) (a) Vainrub, A.; Pettitt, B. M. *Phys. Rev. E* **2002**, *66*, art. no.-041905. (b) Vainrub, A.; Pettitt, B. M. *J. Am. Chem. Soc.* **2003**, *125*, 7798−7799.
(21) (a) Fogleman, E. A.; Yount, W. C.; Xu, J.; Craig, S. L. *Angew. Chem., Int. Ed.* **2002**, *41*, 4026−4028. (b) Xu, J.; Fogleman, E. A.; Craig, S. L. *Macromolecules* **2004**, *37*, 1863−1870. (c) Kim, J.; Liu, Y.; Ahn, S. J.; Zauscher, S.; Karty, J. M.; Yamanaka, Y.; Craig, S. L. *Adv. Mater.* **2005**, *17*, 1749−1753. (d) Kersey, F. R.; Lee, G.; Marszalek, P.; Craig, S. L. *J. Am. Chem. Soc.* **2005**, *127*, 3038−3039.
(22) van der Gucht, J.; Besseling, N. A. M.; Cohen Stuart, M. A. *J. Am. Chem. Soc.* **2002**, *124*, 6202−6205.
(23) Following ref 20b and assuming 100 strands per DNA−Au, ΔG_{diff} at 0.3 M salt is calculated to be 11.9 kcal mol^{-1} (planar surface) versus 4.8 kcal mol^{-1} (nanoparticle) observed experimentally, assuming 50% surface hybridization at T_m measured by DLS. If T_m occurs at 10% surface coverage, the values are 7.6 and 6.1 kcal mol^{-1}, respectively.

specific to the conditions of the measurement. The overarching conclusion of strongly non-Langmuir binding, however, is more general.

Multi-particle aggregates of DNA−Au formed through multiple hybridization events per particle are well-known to be more stable than the isolated duplexes that link the particles,[12] and it is worth pointing out that the results described here are not at odds with the enhanced stability of DNA−Au aggregates. The creation of additional cooperative bridging duplexes between nanoparticles can still add to the stability of an aggregate, even if those additional duplexes are less stable than their isolated counterparts. We observe, for example, that aggregates formed from the exact same **GC-1** + **4** components described above display the same enhanced stability characteristic of the DNA−Au systems, in general (Supporting Information). The results presented here, therefore, reveal another layer of complexity in an already complicated relationship between aggregate stability and the structure of the DNA−Au and target strand components.[12] Ongoing studies should further refine a complete view of hybridization thermodynamics on DNA−Au surfaces.

Conclusion

In conclusion, duplexes on the surface of nonaggregated DNA-functionalized gold colloids become progressively less stable as the fraction of hybridized DNA on the surface increases. The destabilization relative to identical duplexes in solution is greater for longer sequences and represents another layer of complexity in the thermodynamics underlying DNA-directed nanoparticle assembly and detection, particularly in cases where surface hybridization is either prevalent or localized. The present findings also facilitate studies, using DNA-based systems,[21] of colloidal forces from surface-tethered reversible polymers.[22] The surface structure on nanoparticles differs from that on planar surfaces because of the relatively high curvature; in the systems examined here, the surface area per molecule at the DNA−Au periphery is approximately twice that at the gold surface. Nonetheless, electrostatic interactions between DNA have a dramatic effect on the thermodynamics of hybridization.

Acknowledgment. We thank the Petroleum Research Fund of the American Chemical Society, Duke University, the North Carolina Biotechnology Center and Research Corp. for financial support. S.L.C. gratefully acknowledges a DuPont Young Professor Award and a Camille and Henry Dreyfus New Faculty Award, and J.X. acknowledges a Burroughs-Wellcome Fellowship. We thank A. Lytton-Jean and C. Mirkin for helpful discussions and for providing a sample of **GC-3**, and M. Schmidt for thoughtful conversations.

Supporting Information Available: Additional data from the UV and DLS melting curves, thermodynamic treatments, and aggregation study. This material is available free of charge via the Internet at http://pubs.acs.org.

JA052352H